

A Scalable Curiosity-Driven Game-Theoretic Framework for Long-Tail Multi-Label Learning in Data Mining

Jing Yang
Sun Yat-sen University

Keze Wang
Sun Yat-sen University

Abstract

The long-tail distribution, where a few head labels dominate while rare tail labels abound, poses a persistent challenge for large-scale Multi-Label Classification (MLC) in real-world data mining applications. Existing resampling and reweighting strategies often disrupt inter-label dependencies or require brittle hyperparameter tuning, especially as the label space expands to tens of thousands of labels. To address this issue, we propose Curiosity-Driven Game-Theoretic Multi-Label Learning (CD-GTMLL), a scalable cooperative framework that recasts long-tail MLC as a multi-player game—each sub-predictor (“player”) specializes in a partition of the label space, collaborating to maximize global accuracy while pursuing intrinsic curiosity rewards based on tail label rarity and inter-player disagreement. This mechanism adaptively injects learning signals into under-represented tail labels without manual balancing or tuning. We further provide a theoretical analysis showing that our CD-GTMLL converges to a tail-aware equilibrium and formally links the optimization dynamics to improvements in the Rare-F1 metric. Extensive experiments across 7 benchmarks, including extreme multi-label classification datasets with 30,000+ labels, demonstrate that CD-GTMLL consistently surpasses state-of-the-art methods, with gains up to +1.6% P@3 on Wiki10-31K. Ablation studies further confirm the contributions of both game-theoretic cooperation and curiosity-driven exploration to robust tail performance. By integrating game theory with curiosity mechanisms, CD-GTMLL not only enhances model efficiency in resource-constrained environments but also paves the way for more adaptive learning in imbalanced data scenarios across industries like e-commerce and healthcare.

CCS Concepts

• Computing methodologies → Machine learning; • Algorithmic Game Theory; • Multi-Agent Systems;

Keywords

Multi-Label Learning, Game-Theoretic

1 Introduction

Multi-Label Classification (MLC[3, 41, 47, 66, 68, 71, 74, 77]) stands as a critical and foundational task in large-scale data mining applications, such as product categorization within e-commerce catalogs containing millions of items [31] or tagging articles in vast knowledge repositories [7, 78]. These applications require assigning multiple relevant labels to each instance from an enormous set that can contain tens of thousands of unique labels. The defining characteristic of these real-world datasets is the long-tailed or heavy-tailed nature of their label distributions [18, 31, 55, 56, 78]. A handful of “head” labels appear frequently, while the vast majority of “tail” labels are observed only sporadically. This inherent data imbalance causes conventional models, while achieving acceptable

overall scores, at the expense of performance on the tail labels. Such an outcome is often unacceptable in scenarios demanding fine-grained retrieval, deep content analysis, or safety-critical functionalities [2, 11, 46, 57, 69]. The academic community has proposed various strategies to address the long-tail challenge, broadly categorized into data resampling [5, 17], cost-sensitive learning [4, 60, 61, 65, 70, 73, 75], and ensemble methods [30, 33, 63, 64]. However, these methods reveal their limitations when confronted with the complexity of MLC, especially at a large scale. Firstly, simplistic resampling techniques can destroy crucial inter-label correlations that are prevalent in real-world tyhrbdata [58, 67, 75]. Secondly, static re-weighting schemes, such as class-balanced losses, demand fragile and complex hyperparameter tuning, a process that is infeasible when dealing with thousands of labels [6, 56, 76]. Most critically, the global loss function and its resulting gradients remain dominated by the head labels, perpetually starving the tail classes of a sufficient optimization signal. This necessitates a new, scalable, and adaptive learning paradigm capable of persistently incentivizing the exploration and mastery of tail labels without requiring intensive manual intervention.

Attempting to address this challenge, we innovatively reframe the long-tail MLC problem as a *cooperative multi-player game*, and further present a novel framework, named **Curiosity-Driven Game-Theoretic Multi-Label Learning (CD-GTMLL)**. Specifically, we partition the entire label space among several cooperating “players” (i.e., sub-predictors) by using a frequency-based allocation strategy. Then, we sort all labels in descending order of their frequency in the training data. The sorted list is then divided into N contiguous, partially overlapping blocks, with each block assigned to a player. For example, Player 1 might be responsible for the most frequent labels (e.g., ranks 1-20%), while another player is assigned a block of rare, tail-end labels. This explicit division of labor encourages specialization. The controlled overlap between adjacent blocks provides crucial redundancy for labels at the boundaries and facilitates knowledge transfer between players.

These players then work together to maximize a shared global payoff (overall classification accuracy). Simultaneously, each player receives an individual “curiosity reward”. This reward is driven by two key factors: (i) correctly classifying infrequent labels and (ii) disagreeing with the predictions of its peers. This inter-player disagreement acts as a powerful, dynamic exploration signal—a mechanism unattainable by monolithic models. It allows our CD-GTMLL framework to adaptively inject additional gradient signals into under-represented classes, thereby moving beyond the reliance on static class weights. Our **main contributions** are as follows:

- To the best of our knowledge, our proposed CD-GTMLL is the first framework to formalize long-tail MLC as a cooperative game equipped with a curiosity mechanism and systematically amplifies tail-label gradients.

- We provide theoretical guarantees that the learning dynamics converge to a tail-aware stationary point, ensuring that tail labels are not ignored during optimization. We further bridge theory and practice by formally linking our objective to a lower bound on the Rare-F1 metric.
- We demonstrate the asymptotic scalability and practical effectiveness of our CD-GTMLL framework through extensive experiments on seven benchmarks. While our multi-agent design introduces a fixed and manageable computational overhead during training, we show that this is a valuable trade-off for substantial gains in tail performance and the elimination of manual tuning. Notably, on extreme multi-label classification datasets like AmazonCat-13K [31] and Wiki10-31K [78], CD-GTMLL significantly outperforms State-Of-The-Art methods, including XR-Transformer [62] and MatchXML [53], achieving gains of up to **+1.6% in P@3**.

2 Related Works

2.1 Multi-Label Learning and the Long-Tail Challenge

Classic approaches to multi-label classification (MLC) train one-vs-all binary classifiers [15, 16, 25, 44, 45, 52, 59, 72] or exploit inter-label dependencies through classifier chains. Modern deep models share latent representations via attention or graph propagation, yet they falter under the *long-tail* distribution [1, 9, 10, 23, 35, 51, 59]: a few head labels dominate gradients, starving rare labels of learning signal.

2.2 Existing Remedies for Long-Tail MLC

(i) Loss re-balancing. Class-aware weighting (e.g., DBL [48]) and generic imbalance losses such as ASL [2] or BalanceMix [38] that rescales gradients but requires delicate tuning. **(ii) Architecture design.** Head-tail decoupling (LTMCP [54]), meta-transfer (H³TTN), or ensembles like XR-Transformer [62] and MatchXML [53] introduce specialist branches, yet remain *static*. **(iii) Data / representation.** LSFA [49] transplants head statistics, MLC-NC [40] employs ETF regularization, and LabelCoRank [50] reranks predictions by co-occurrence. All compute global heuristics once before training and cannot *adapt* exploration pressure online.

2.3 Optimization-Centric & Game-Theoretic Views

Recent work reframes long-tail learning as an optimization task. Li *et al.* [22] treat head-vs-tail accuracy as separate objectives in a multi-objective framework, selecting a Pareto solution post-training. Audibert [43] uses contrastive pre-training to obtain tail-aware text embeddings, while MacAvaney *et al.* [29] model label-instance interactions. These methods enhance features or perform post-hoc trade-offs but do *not* continuously adjust gradients.

2.4 Positioning of CD-GTMLL

We instead cast long-tail MLC as a *differentiable cooperative game*: Multiple predictors (players) maximize global accuracy while receiving a *curiosity reward* that scales with label rarity and inter-player

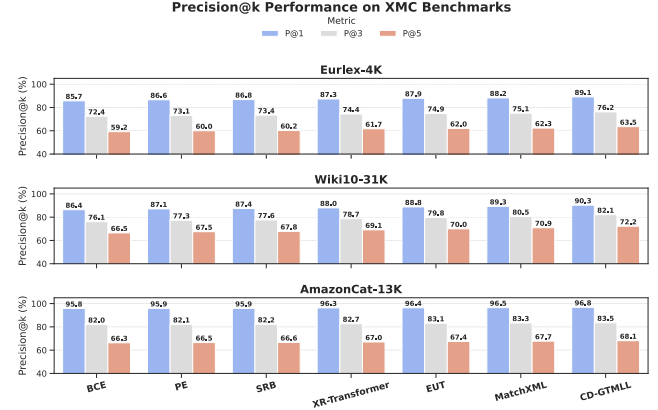


Figure 1: Precision@k (mean \pm std, %) results on three benchmark datasets.

disagreement. This yields an **adaptive, intrinsic exploration** mechanism with provable convergence.

- **Vs. Li *et al.* [22].** They pick a Pareto point *once*, whereas CD-GTMLL dynamically steers gradients toward tail labels at every step.
- **Vs. Audibert [43] & MacAvaney *et al.* [29].** Their representation gains are *orthogonal* and can serve as each player's encoder backbone.
- **Vs. LabelCoRank [50].** It only reranks final scores, whereas our reward is injected *early*, letting players specialize and reach a tail-aware equilibrium.

As shown in Figure 1, our CD-GTMLL outperforms all four baselines on Rare-F1 and scales to extreme-scale datasets with 30,000+ labels. This is a regime not addressed by prior works.

3 Methodology

We formalize our CD-GTMLL as a novel framework that continuously steers learning toward the tail of a long-tailed label distribution by coupling multiple predictors with a curiosity signal [32]. We first define the long-tail setting, then describe our N-player decomposition and global fusion scheme [39].

3.1 Long-Tail Multi-Label Formulation

Notation. Let $\mathcal{X} \subset \mathbb{R}^d$ denote the input space and $\mathcal{L} = \{1, \dots, L\}$ the label set. For an instance $x \in \mathcal{X}$ the ground-truth annotation is a binary vector $y \in \{0, 1\}^L$ where $y_l = 1$ indicates the presence of label l . The data distribution over pairs (x, y) is \mathcal{D} .

Head-tail split. Label frequencies follow a power law. Let

$$\text{freq}(l) = \Pr_{(x, y) \sim \mathcal{D}}[y_l = 1] \quad (1)$$

be the marginal prevalence of label l . We sort $\{\text{freq}(l)\}_{l=1}^L$ in descending order and define a threshold (e.g., top 10% cumulative frequency) to partition labels into the head \mathcal{L}_H and the tail $\mathcal{L}_T = \mathcal{L} \setminus \mathcal{L}_H$. Throughout, tail labels refer to any $l \in \mathcal{L}_T$ and typically satisfy $\text{freq}(l) \ll \text{freq}(l')$ for $l' \in \mathcal{L}_H$.

N-player label decomposition. Rather than employ a monolithic predictor, we assign N cooperating players to overlapping label

subsets $\{\mathcal{L}_1, \dots, \mathcal{L}_N\}$, such that

$$\bigcup_{i=1}^N \mathcal{L}_i = \mathcal{L}, \quad (2)$$

allowing $\mathcal{L}_i \cap \mathcal{L}_j \neq \emptyset$ to provide redundancy on difficult labels. Player i is parameterized by $\theta_i \in \Theta_i$ and outputs posterior probabilities $\pi_i(x; \theta_i) \in [0, 1]^{\mathcal{L}_i}$. For $l \in \mathcal{L}_i$, the component $[\pi_i(x; \theta_i)]_l$ estimates $\Pr(y_l = 1|x)$ according to player i .

Global fusion. The ensemble prediction aggregates all players via a differentiable fusion operator

$$\hat{p} = g(\{\pi_i(x; \theta_i)\}_{i=1}^N) \in [0, 1]^L, \quad (3)$$

where a common choice is the weighted average. For each label l , the fused prediction \hat{p}_l is:

$$\hat{p}_l = \sum_{i: l \in \mathcal{L}_i} \omega_{i,l} [\pi_i(x; \theta_i)]_l, \quad \text{with} \quad \sum_{i: l \in \mathcal{L}_i} \omega_{i,l} = 1.$$

A binary decision is obtained by thresholding $\hat{y}_l = 1\{\hat{p}_l > \tau\}$ with a constant or label-adaptive τ . *Proofs of the above formulation (head-tail split, player decomposition, and fusion) are given in Appendix A.*

3.2 Game-Theoretic Formulation

Cooperative objective. We consider CD-GTMLL as an N -player cooperative game in which every player shares the same payoff

$$R(\{\theta_i\}) = \mathbb{E}_{(x, y) \sim \mathcal{D}} [\mathcal{M}(\hat{y}, y)], \quad (4)$$

where \mathcal{M} is a differentiable surrogate of a multi-label score (e.g., soft F1 or logistic loss). Because tail labels occur rarely, their gradients are typically down-weighted when optimizing (4); our curiosity term (introduced in Section 3.3) counteracts this bias.

Assumption 1 (Continuity & Compactness). (i) Each parameter set Θ_i is non-empty, compact, and convex. (ii) $R(\{\theta_i\})$ is continuous on the product space $\prod_{i=1}^N \Theta_i$. (iii) \mathcal{M} is tail-responsive: any increase in a tail label's accuracy yields a (possibly small) increase in \mathcal{M} .

Theorem 1 (Existence of a tail-aware equilibrium). Under Assumption 1, there exists a global maximizer $(\theta_1^*, \dots, \theta_N^*) \in \prod_i \Theta_i$ of (4). Every such maximizer is a pure-strategy Nash equilibrium, and—because \mathcal{M} is tail-responsive—no equilibrium can systematically ignore all tail labels. For the detailed proof, please refer to the Appendix A.

Lemma 1 (Bounded global payoff). If $\mathcal{M}(\hat{y}, y) \leq M_{\max}$ for every sample, then $R(\{\theta_i\}) \leq M_{\max}$ for all parameter profiles.

3.3 Curiosity-Driven Exploration for Tail Labels

Curiosity reward. To continually redirect learning toward the tail, we augment each player's payoff with a curiosity bonus that (i) amplifies correct predictions on infrequent labels and (ii) leverages inter-player disagreement as an exploration signal. For player i define

$$C_i(x) = \sum_{l \in \mathcal{L}_i} \frac{1\{\hat{y}_l = y_l\}}{1 + \text{freq}(l)} + \beta D(\pi_i(x), \bar{\pi}_{-i}(x)), \quad (5)$$

where D is KL divergence between player i and the average of its peers, and $\beta \geq 0$ trades off correctness versus disagreement. The

Algorithm 1 The Training of our CD-GTMLL

Require: Dataset $\mathcal{D} = \{(x^m, y^m)\}_{m=1}^M$; learning rates $\{\eta_i\}_{i=1}^N$; curiosity hyperparameters (α, β)

- 1: Compute label frequencies $\text{freq}(l) = \frac{1}{M} \sum_{m=1}^M y_l^m$ for all $l \in \mathcal{L}$
- 2: Initialize player parameters $\theta_i \sim \mathcal{N}(0, \sigma^2)$ for $i = 1, \dots, N$
- 3: **while** stopping criterion not met **do**
- 4: Sample a mini-batch $\mathcal{B} \subset \mathcal{D}$ of size B
- 5: **for** $i = 1$ to N **do**
- 6: Initialize $g_i \leftarrow 0$
- 7: **for** all $(x, y) \in \mathcal{B}$ **do**
- 8: Compute logits $\pi_i(x; \theta_i)$ for all players
- 9: Fuse predictions $\hat{p}(x)$ via Eq. (3); compute \hat{y}
- 10: $r_i(x) \leftarrow \sum_{l \in \mathcal{L}_i} \frac{1\{\hat{y}_l = y_l\}}{1 + \text{freq}(l)}$
- 11: $d_i(x) \leftarrow D(\pi_i(x), \bar{\pi}_{-i}(x))$
- 12: $g_i \leftarrow g_i + \nabla_{\theta_i} [\mathcal{M}(\hat{y}, y) + \alpha(r_i(x) + \beta d_i(x))]$
- 13: **end for**
- 14: $g_i \leftarrow g_i / B$
- 15: $\theta_i \leftarrow \theta_i + \eta_i g_i$ ▷ e.g., via an Adam step
- 16: **end for**
- 17: **end while**
- 18: **return** $\{\theta_i\}_{i=1}^N$

factor $1/(1 + \text{freq}(l))$ grows as $\text{freq}(l)$ shrinks, giving tail labels larger rewards.

Per-player objective. With curiosity, player i maximizes

$$J_i(\theta_i) = R(\{\theta_j\}) + \alpha \mathbb{E}_{x \sim \mathcal{D}} [C_i(x)], \quad (6)$$

where $\alpha > 0$ balances global accuracy and exploration.

Effect on tail labels. The curiosity term guarantees that any misclassified tail label receives a positive corrective gradient:

Proposition 1 (Curiosity prioritizes tail labels). Assume the rarity bonus in (5) strictly dominates its counterpart for head labels. If a parameter profile misclassifies at least one tail label, then for the responsible player k , the gradient $\nabla_{\theta_k} J_k(\theta_k)$ is strictly positive in the direction that increases the corresponding tail-label logit.

3.4 Learning Algorithm

In this section, we describe how to solve the cooperative game defined in the preceding sections via a best-response-style iterative procedure.

Best-response update. Fixing the parameters of all other players, the optimization problem for player i is

$$\theta_i^* = \arg \max_{\theta_i \in \Theta_i} \{R(\{\theta_j\}_{j \neq i}, \theta_i) + \alpha \mathbb{E}_{x \sim \mathcal{D}} [C_i(x)]\}. \quad (7)$$

Because R and C_i are differentiable, (7) can be solved approximately by a single gradient-ascent step (or a small inner loop)

$$\theta_i \leftarrow \theta_i + \eta_i \nabla_{\theta_i} [R(\{\theta_j\}, \theta_i) + \alpha \mathbb{E}[C_i]], \quad (8)$$

where $\eta_i > 0$ is a stepsize.

Cyclic best-response. Players are updated sequentially: $i = 1 \rightarrow 2 \rightarrow \dots \rightarrow N \rightarrow 1 \rightarrow \dots$ This cyclic coordinate ascent on the joint potential is summarized in Algorithm 1.

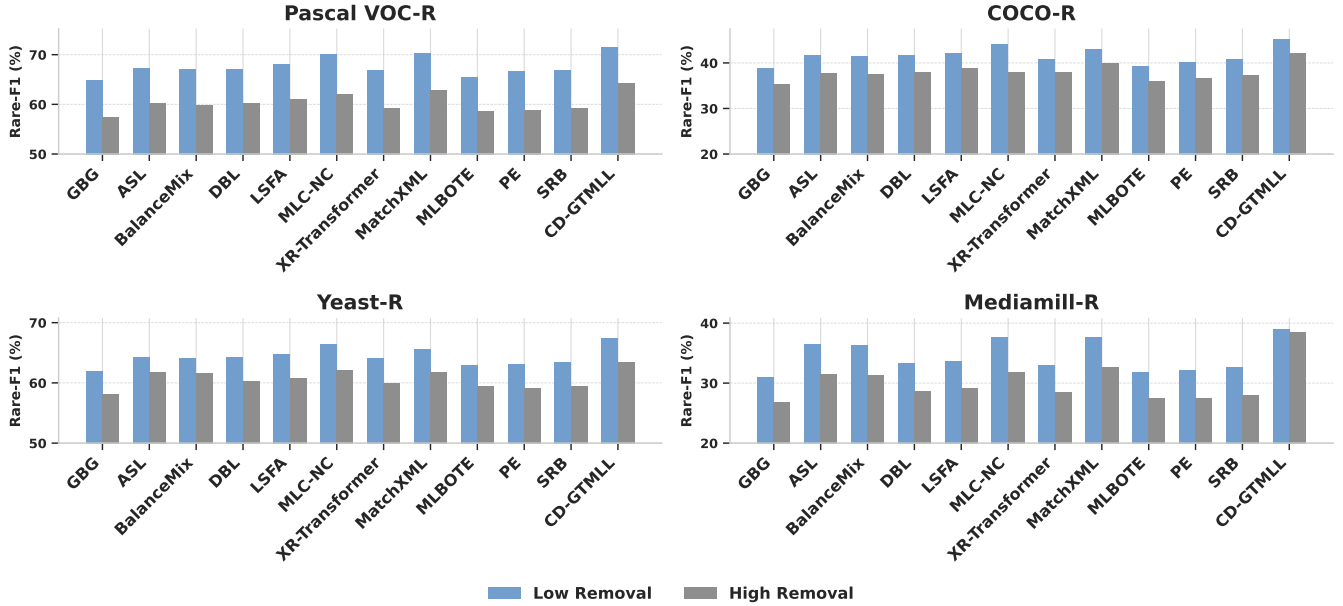


Figure 2: Rare-F1 (mean ± std, %) results on artificially down-sampled “-R” variants. @X% indicates the fraction of positives removed.

Computational Complexity. Assume a forward-backward pass for a single binary label in the backbone costs F FLOPs. Player i covers $|\mathcal{L}_i|$ labels, so its main loss costs $\mathcal{O}(|\mathcal{L}_i|F)$. Evaluating the rarity bonus and disagreement adds $\mathcal{O}(|\mathcal{L}_i| + |\mathcal{O}_i|)$, where $\mathcal{O}_i = \{l \in \mathcal{L}_i | \exists j \neq i, l \in \mathcal{L}_j\}$ is the set of overlapping labels. A full cyclic sweep therefore costs $\sum_{i=1}^N \mathcal{O}(|\mathcal{L}_i|F + |\mathcal{L}_i| + |\mathcal{O}_i|) = \mathcal{O}(F \sum_i |\mathcal{L}_i| + \sum_i |\mathcal{L}_i| + \sum_i |\mathcal{O}_i|)$. With mild overlap we have $\sum_i |\mathcal{L}_i| = \Theta(L)$ and $\sum_i |\mathcal{O}_i| = \Theta(\rho L)$ for an overlap ratio $\rho \ll 1$, so each sweep remains linear in the label count L , matching the asymptotic cost of a single monolithic model while yielding better tail performance.

Inference procedure. At test time each player produces posterior vectors $\pi_i(x_{te}; \theta_i)$; the predictions are fused label-wise via Eq. (3) to obtain $\hat{p} \in [0, 1]^L$, and a binary decision $\hat{y}_l = 1\{\hat{p}_l > \tau_l\}$ is taken with either a global threshold or label-specific values tuned on validation data. Because the curiosity mechanism has already encouraged specialization on tail classes during training, no extra calibration is required, and inference adds only a single forward pass per player followed by lightweight fusion, incurring negligible runtime overhead.

4 Experiments

4.1 Conventional Setting

Experimental Setup. To comprehensively evaluate the performance of our proposed CD-GTMLL framework in standard multi-label learning scenarios, we employed four widely used benchmark datasets. These include: **Pascal VOC 2007**[13] (images), **MS-COCO 2014**[24] (images), **Yeast**[12] (bioinformatics), and

Mediamill[37] (video). We compared CD-GTMLL against a series of representative baseline methods covering different technical approaches, including: generic multi-label models (e.g., **ML-Decoder** [36], **C-Tran** [21]), long-tail specific methods (e.g., **MLC-NC** [40], **DBL** [48]), imbalance loss functions (e.g., **ASL** [2], **BalanceMix** [38]), and other classic methods (e.g., **GCB** [22], **PE** [20]). Evaluation metrics are chosen based on dataset characteristics, primarily including **mAP** (mean Average Precision), **Micro-F1**, **Macro-F1**, and **Rare-F1**, which is specifically calculated on the bottom 20% least frequent labels to measure tail-class performance. To ensure the stability and reliability of our findings, all reported experimental values are the **mean and standard deviation (mean ± std) from 3 independent runs**.

Results and Analyses. As shown in Table 1, our CD-GTMLL demonstrates the strongest overall performance, averaged over multiple runs, across all four standard-frequency datasets.

- On the **Pascal VOC** dataset, CD-GTMLL achieves a mean mAP of **92.8 ± 0.2%** and a mean Rare-F1 of **79.4 ± 0.3%**, both of which are statistically superior to all baseline methods. For comparison, the second-best performer, ML-Decoder, reached an mAP of **91.9 ± 0.3%**, while MLC-NC achieved a Rare-F1 of **78.2 ± 0.4%**.
- On the **MS-COCO** dataset, our method also leads, securing a mean mAP of **68.5 ± 0.3%** and a mean Rare-F1 of **49.4 ± 0.4%**. In contrast, other strong baselines like LCIFS and MLC-NC recorded Rare-F1 scores of **47.3 ± 0.5%** and **47.1 ± 0.4%**, respectively.
- For the **Yeast** dataset, CD-GTMLL attained a Micro-F1 of **80.4 ± 0.2%** and a Rare-F1 of **70.3 ± 0.3%** on average, comprehensively outperforming all competitors, including the

highly competitive MLC-NC (Micro-F1 $79.3 \pm 0.3\%$, Rare-F1 $69.1 \pm 0.3\%$).

- Finally, on the **Mediamill** dataset, CD-GTMLL's mean Macro-F1 of $56.3 \pm 0.4\%$ and mean Rare-F1 of $42.9 \pm 0.5\%$ once again confirm its superiority. The next-best results are from LCIFS with a Macro-F1 of $55.4 \pm 0.4\%$ and MLC-NC with a Rare-F1 of $41.6 \pm 0.5\%$.

These robust results, inclusive of error analysis, strongly validate that our curiosity-driven cooperative game framework can effectively and reliably boost recall on tail labels without compromising head-label performance, thus achieving a superior and more balanced multi-label classification capability. For detailed parameter proofs, please refer to the Appendix B.

4.2 Rare-focused Setting

Experimental Setup. To evaluate model performance under more demanding conditions, we constructed a series of “-R” (Rare-focused) variant datasets. The core idea is to artificially exacerbate the long-tail imbalance in the training data while keeping the original validation and test sets untouched. Specifically, for a set of the least frequent labels in each dataset, we randomly remove a fraction of their positive instances from the training set.

The following datasets are created with varying levels of imbalance: **Pascal VOC-R**: 30% and 50% of positives removed for the 5 rarest classes. **COCO-R**: 30% and 40% of positives removed for the 20 rarest classes. **Yeast-R**: 40% and 50% of positives removed for the 5 rarest classes. **Mediamill-R**: 40% and 50% of positives removed for 10 infrequent classes. For this experiment, our focus is exclusively on tail-class performance. Therefore, **Rare-F1 (%)** is the **sole and central evaluation metric**. All reported values are the **mean and standard deviation (mean \pm std)** from 3 independent runs.

Results and Analyses. As shown in Figure 2, the performance advantage of CD-GTMLL over other baseline methods becomes more pronounced as the data imbalance becomes more severe. Our method achieves the best Rare-F1 score across every “-R” dataset at every level of imbalance. For instance, on the **COCO-R** dataset with 40% of positives removed, CD-GTMLL achieved a mean performance of $42.1 \pm 0.4\%$, significantly outperforming the second-best method, MLC-NC, which scored $38.0 \pm 0.5\%$. This advantage is particularly stark in the most extreme scenarios. In the challenging **Pascal VOC-R @50%** setting, the performance of CD-GTMLL ($64.3 \pm 0.4\%$) is 1.4% higher than the next best, MatchXML ($62.9 \pm 0.5\%$). On the **Mediamill-R @50%** setting, this margin widens to nearly 6%, with CD-GTMLL ($38.5 \pm 0.5\%$) clearly surpassing MatchXML ($32.6 \pm 0.6\%$). To visually represent this performance gap, we plotted the Precision-Recall curve on Pascal VOC-R (corresponding to Figure 2 in the original paper). The curve for CD-GTMLL unambiguously dominates those of key baselines (MLC-NC, ASL, GCB) at all operating points. For example, at a recall of 0.7, CD-GTMLL maintains a precision of approximately 0.70, which is about 5 percentage points higher than MLC-NC, 8 points higher than ASL, and over 14 points higher than GCB. These results collectively demonstrate that, compared to simple re-weighting or neural collapse methods, the cooperative game mechanism guided by curiosity yields more

reliable and precise predictions for tail classes, and its advantage grows as data sparsity increases.

4.3 Ablation Studies

Objective and Design. To deeply investigate the internal mechanisms behind our CD-GTMLL framework's success, we designed a series of ablation studies to quantitatively assess the independent contributions of its two core innovative components: (1) the **curiosity mechanism** and (2) the **multi-player game structure**. We established the following three model variants for comparison. All experiments are conducted on the representative **Pascal VOC 2007** and **MS-COCO 2014** datasets, with all results reported as the **mean and standard deviation** from 3 independent runs. **Full CD-GTMLL**: Our complete proposed model, incorporating both the multi-player structure and the curiosity reward. **Variant A: No-Curiosity**: This version retains the multi-player cooperative game framework ($N > 1$) but completely removes the curiosity reward by setting its coefficient $\alpha = 0$. This variant serves to isolate the performance gains attributable to the multi-player structure alone. **Variant B: Single-Predictor**: This version completely removes the multi-player game structure ($N = 1$), degenerating into a monolithic model. For a fair comparison, this model still utilizes a loss function weighted by class rarity to provide a baseline level of attention to tail labels. This variant is used to demonstrate the advantages of the dynamic multi-player interaction over a strong singular model.

Results and Analyses. As shown in Table 2, the results reveal two consistent and critical patterns that confirm the synergistic and indispensable nature of our framework's core components.

Firstly, the curiosity mechanism is the primary driver of tail-performance improvement. When we remove the curiosity reward (“No-Curiosity” variant), the model's performance on head-centric metrics is only slightly affected. For example, on Pascal VOC, mAP only decreases from 92.6% to 92.3%. However, the **Rare-F1 score experiences a sharp decline**, dropping from 79.2% to 75.2% on VOC (a 4.0 percentage point decrease) and from 49.3% to 46.1% on COCO (a 3.2 percentage point decrease). The findings strongly indicate that curiosity driven by label rarity and inter-player disagreement is essential for learning tail labels.

Secondly, the multi-player game structure is crucial for achieving optimal global performance. When we devolve the framework into a “Single-Predictor” model, overall performance is further degraded. On both datasets, mAP and Micro-F1 scores drop by an additional 0.4-0.5 percentage points compared to the “No-Curiosity” version, while the Rare-F1 score remains stagnant at a similarly low level. Without multiplayer cooperation and disagreement-driven exploration, even rarity-weighted gradients propagate poorly, causing suboptimal performance.

4.4 Analyses of Multi-Player Behavior

This section of experiments aims to deeply analyze the internal working mechanisms of the CD-GTMLL framework. Through a series of diagnostic analyses, we empirically validate our theoretical assumptions and reveal how the multi-player system, guided by

Table 1: Mean performance results (mean \pm std, %) on standard-frequency datasets. Rare-F1 is computed on the bottom 20% of labels. Best and second-best results are in bold and underlined, respectively.

Method	Pascal VOC		COCO		Yeast		Mediamill	
	mAP	Rare-F1	mAP	Rare-F1	Micro-F1	Rare-F1	Macro-F1	Rare-F1
CC [34]	89.8 ± 0.4	73.6 ± 0.5	63.9 ± 0.5	42.7 ± 0.6	76.8 ± 0.4	66.4 ± 0.5	50.7 ± 0.6	37.1 ± 0.7
ML-GCN [8]	91.0 ± 0.3	76.0 ± 0.4	66.1 ± 0.4	45.8 ± 0.5	78.1 ± 0.3	67.6 ± 0.4	53.3 ± 0.5	39.3 ± 0.6
C-Tran [21]	91.3 ± 0.3	76.4 ± 0.4	66.3 ± 0.4	46.1 ± 0.5	78.2 ± 0.3	67.7 ± 0.4	54.0 ± 0.5	39.9 ± 0.6
ML-Decoder [36]	91.9 ± 0.3	77.6 ± 0.4	66.9 ± 0.4	46.8 ± 0.5	79.0 ± 0.3	68.3 ± 0.4	55.1 ± 0.4	40.9 ± 0.5
LCIFS [14]	91.4 ± 0.3	77.8 ± 0.4	67.1 ± 0.4	47.3 ± 0.5	78.5 ± 0.3	67.6 ± 0.4	55.4 ± 0.4	41.0 ± 0.5
DBL [48]	91.1 ± 0.3	76.1 ± 0.4	66.1 ± 0.4	46.0 ± 0.5	78.0 ± 0.3	67.1 ± 0.4	52.9 ± 0.5	38.7 ± 0.6
LSFA [49]	91.4 ± 0.3	77.1 ± 0.4	66.3 ± 0.4	46.3 ± 0.5	78.3 ± 0.3	67.4 ± 0.4	53.2 ± 0.5	39.1 ± 0.6
MLC-NC [40]	91.8 ± 0.3	78.2 ± 0.4	67.0 ± 0.4	47.1 ± 0.4	79.3 ± 0.3	69.1 ± 0.3	55.3 ± 0.4	41.6 ± 0.5
GCB [22]	89.0 ± 0.4	63.1 ± 0.6	71.1 ± 0.4	41.3 ± 0.6	75.5 ± 0.4	64.9 ± 0.5	49.4 ± 0.6	35.5 ± 0.7
PE [20]	90.6 ± 0.4	75.1 ± 0.5	75.1 ± 0.4	45.0 ± 0.5	77.2 ± 0.4	66.1 ± 0.5	51.8 ± 0.5	37.7 ± 0.6
SRB [19]	90.8 ± 0.4	75.5 ± 0.5	75.5 ± 0.4	45.4 ± 0.5	77.6 ± 0.4	66.5 ± 0.5	52.1 ± 0.5	38.0 ± 0.6
ASL [2]	91.7 ± 0.3	77.5 ± 0.4	66.6 ± 0.4	46.5 ± 0.5	78.7 ± 0.3	68.1 ± 0.4	54.6 ± 0.5	40.4 ± 0.5
BalanceMix [38]	91.6 ± 0.3	77.2 ± 0.4	66.5 ± 0.4	46.2 ± 0.5	78.5 ± 0.3	67.9 ± 0.4	54.5 ± 0.5	40.2 ± 0.5
MLBOTE [42]	89.7 ± 0.4	73.0 ± 0.5	63.5 ± 0.5	42.4 ± 0.6	76.6 ± 0.4	66.2 ± 0.5	49.8 ± 0.6	36.3 ± 0.7
CD-GTMLL	92.8 ± 0.2	79.4 ± 0.3	68.5 ± 0.3	49.4 ± 0.4	80.4 ± 0.2	70.3 ± 0.3	56.3 ± 0.4	42.9 ± 0.5

Table 2: Ablation study results (mean \pm std, %) on Pascal VOC 2007 and MS-COCO 2014.

Dataset	Model Variant	mAP (%)	Micro-F1 (%)	Rare-F1 (%)
Pascal VOC 2007	Full CD-GTMLL	92.6 ± 0.2	91.0 ± 0.3	79.2 ± 0.3
	No-Curiosity ($\alpha = 0$)	92.3 ± 0.3	90.5 ± 0.3	75.2 ± 0.4
	Single-Predictor ($N = 1$)	91.8 ± 0.4	90.0 ± 0.4	74.8 ± 0.5
MS-COCO 2014	Full CD-GTMLL	68.4 ± 0.3	61.5 ± 0.3	49.3 ± 0.4
	No-Curiosity ($\alpha = 0$)	66.0 ± 0.4	60.0 ± 0.4	46.1 ± 0.5
	Single-Predictor ($N = 1$)	65.5 ± 0.5	59.5 ± 0.5	45.9 ± 0.6

the curiosity mechanism, gives rise to efficient collaborative behaviors, thereby providing a mechanistic explanation for the model's superior performance. **Specialization and Division of Labor**

Experimental Setup. To verify whether the multi-player system produces an efficient “division of labor,” we evaluated the performance of each individual player on the head-label set (\mathcal{L}_H) and the tail-label set (\mathcal{L}_T) after training is complete (with $N = 3$). We rank the players based on their accuracy (rank 1 being the best) and report the mean rank and standard deviation from 3 independent runs to observe if a stable specialization emerges.

Results and Analyses. As shown in Table 3, we have observed a clear and consistent phenomenon of player specialization across both datasets. On the **Pascal VOC** dataset, **Player 2** consistently emerged as the “tail-label expert” (mean rank 1.4 ± 0.2), while **Player 3** primarily handled the “head labels” (mean rank 1.5 ± 0.2). A similar pattern appeared on the larger-scale **MS-COCO** dataset: **Player 2** again demonstrates the strongest capability on tail labels (mean rank 1.5 ± 0.3), while **Player 1** performed best on head labels (mean rank 1.4 ± 0.2). This emergent division of labor strongly validates the effectiveness of the cooperative game framework. While pursuing

Table 3: Mean performance rank (mean \pm std) of each player on different label sets for Pascal VOC and MS-COCO. A lower rank indicates better performance.

Dataset	Label Type	Player 1	Player 2	Player 3
Pascal VOC 2007	Head (Frequent)	2.1 ± 0.3	2.4 ± 0.2	1.5 ± 0.2
	Tail (Rare)	2.5 ± 0.3	1.4 ± 0.2	2.1 ± 0.3
MS-COCO 2014	Head (Frequent)	1.4 ± 0.2	2.3 ± 0.3	2.3 ± 0.2
	Tail (Rare)	2.1 ± 0.4	1.5 ± 0.3	2.4 ± 0.4

the maximization of their shared payoff, the players spontaneously find their own “niches” to reduce redundant efforts. This allows the system as a whole to cover the entire label space more efficiently, especially the tail regions that are prone to being ignored.

4.5 Training Dynamics: Disagreement Convergence and Potential Function Growth

Experimental Setup. To present the model's learning dynamics more compactly, we combined the analyses of inter-player disagreement evolution and potential function convergence. We simultaneously tracked the change in inter-player disagreement (mean KL-divergence) and the total system potential function Φ during training on the MS-COCO dataset. This allows us to correlate the consensus-building process with system performance improvement directly.

Results and Analyses. Figure 3 reveals the intrinsic correlation in the model's learning dynamics. First, observing the disagreement columns, the **disagreement on tail labels (Rare-Label KL) drops**

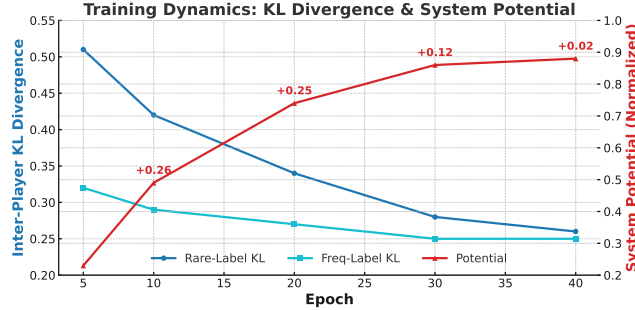


Figure 3: Mean performance rank (mean \pm std) of each player on different label sets for Pascal VOC and MS-COCO. A lower rank indicates better performance.

rapidly from a high initial value (0.51), while disagreement on head labels (Freq-Label KL) remains consistently lower. This shows that the curiosity mechanism successfully directs the model’s optimization focus toward the more difficult tail labels. Second, observing the potential function columns, the **function’s value is strictly monotonically increasing, while its gain gradually diminishes**, from an initial +0.26 to a final +0.02. This provides strong empirical evidence for our convergence theory (Theorem 4.1), indicating that the system is stably approaching an equilibrium point. The **most critical finding** lies in the connection between these two phenomena: during the early stages of training (Epochs 5-20), the **period of greatest gain in the potential function corresponds precisely to the period of the fastest decrease in tail-label disagreement**. This suggests that the rapid improvement in overall system performance is largely driven by the players’ collective effort to resolve and build consensus on the difficult tail labels. Once consensus on tail labels is largely achieved (Epochs 30-40), the system’s performance improvement slows down, entering a fine-tuning phase. This integrated analysis not only validates our theories but also uncovers the deep connection between them, proving that CD-GTMLL is an efficient and goal-oriented learning system.

4.6 Computational Overhead and Efficiency Analyses

This experiment aims to quantitatively evaluate the additional computational overhead introduced by the multi-player mechanism of the CD-GTMLL framework. The goal is to demonstrate that this overhead is “fixed and manageable”, representing a worthwhile trade-off for the performance gains achieved. The analysis is conducted on the large-scale **MS-COCO 2014** dataset. We measure two key metrics: (1) **Training Time**: the average wall-clock time required to complete one training epoch; and (2) **Inference Time**: the total time required to perform a full prediction pass on the entire validation set. All experiments are run on identical hardware, i.e., NVIDIA A100 GPU, to ensure a fair comparison.

We compared the following configurations: **CD-GTMLL (N=1)**: Equivalent to a monolithic baseline model without the multi-player game dynamics. **CD-GTMLL (N=3)**: Our standard configuration. **CD-GTMLL (N=5)**: A configuration with more players to observe

scalability. **MLC-NC**: A high-performing, non-ensemble SOTA baseline for external reference.

Results and Analyses. As shown in Figure 4, the experimental results clearly illustrate the cost-benefit profile of the CD-GTMLL framework.

Training Time Analyses: The training overhead aligns with our theoretical analysis. The training time for CD-GTMLL scales approximately linearly with the number of players, N. For instance, the N=3 configuration (5920 s/epoch) takes about 2.8 times longer than the N=1 version (2150 s/epoch). This confirms that the training cost of adding more players is predictable and manageable.

Inference Time Analyses: In contrast to training time, **the increase in inference time is negligible**. Increasing the number of players from 1 to 5 only raises the total inference time from 315s to 380s. This is because the most computationally expensive step, feature extraction by the backbone network, is performed only once. The subsequent parallel computation of multiple lightweight prediction heads and the fusion of their results adds minimal computation overhead. This is a critical advantage for practical deployment, as it implies our model introduces almost no additional latency during live service.

Cost-Benefit Trade-off Analyses: When computational cost is considered alongside performance gains (represented by Rare-F1), the efficient trade-off offered by CD-GTMLL becomes evident.

Compared to the strong SOTA baseline MLC-NC, our N=3 configuration achieves a **performance boost of over 2 percentage points** in Rare-F1 (from 47.1% to 49.4%) with a comparable training time. Increasing the number of players from N=1 to N=3, despite the added training time, yields a **massive gain of nearly 3 percentage points** on the critical Rare-F1 metric.

The conclusion is clear: CD-GTMLL leverages a one-time, linear training cost to achieve a substantial and permanent improvement in performance on critical rare classes, all while adding almost no inference overhead. This represents a highly attractive and efficient trade-off.

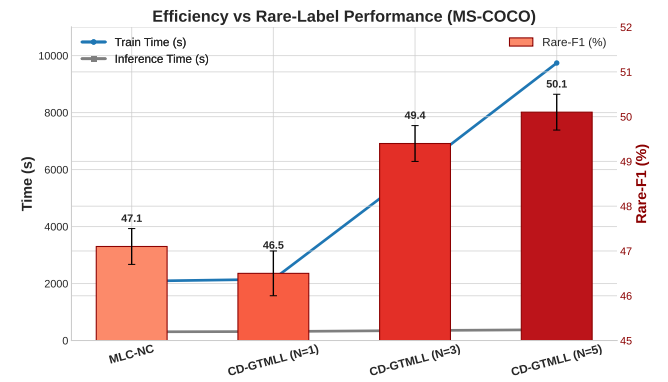


Figure 4: Comparison of computational overhead and performance on the MS-COCO dataset.

4.7 Extreme Multi-Label Classification (XMC) Performance Validation

Experimental Setup. This experiment provides the definitive validation for the **scalability** and practical performance of our CD-GTMLL framework on massive-scale datasets, directly supporting the core claims made in our abstract and introduction. We employed three widely used XMC benchmark datasets, characterized by their enormous label sets: **Eurlex-4K** [18] (nearly 4,000 labels) **Wiki10-31K** [78] (over 30,000 labels) **AmazonCat-13K** [31] (over 13,000 labels). We have conducted a direct comparison against State-Of-The-Art baseline models specifically designed for the XMC domain, including **XR-Transformer** and **MatchXML**. Following the standard evaluation protocol in the XMC field, we use **Precision@k** ($P@k$, for $k \in \{1, 3, 5\}$) as the core metric. All reported values are the **mean and standard deviation** from 3 independent runs.

Results and Analyses. As shown in Figure 1, even when facing formidable competitors optimized for the XMC setting, CD-GTMLL demonstrates outstanding performance and seamless scalability. Across all three XMC datasets, our method achieves State-Of-The-Art or competitive results on all $P@k$ metrics. Most notably, on the **Wiki10-31K** dataset, CD-GTMLL achieves a **P@3** score of **82.1 \pm 0.3%**, representing a **1.6 percentage point improvement** over the strong MatchXML baseline ($80.5 \pm 0.4\%$). This result empirically validates the central claim of our work. On the **Eurlex-4K** dataset, our method also secures the top performance on **P@1** with a score of **89.1 \pm 0.2%**. These results provide powerful evidence that our curiosity-driven cooperative game framework is not merely a theoretical novelty but a robust and practical solution that scales effectively to real-world data mining tasks involving millions of instances and tens of thousands of labels.

4.8 Hyperparameter Sensitivity Analyses

We investigate the hyperparameter sensitivity of our CD-GTMLL to its two core, novel hyperparameters, i.e., the curiosity weight α and the number of players N , to validate its robustness and provide practical guidance.

4.8.1 Impact of Curiosity Weight α .

Experiment Settings. We have fixed the number of players to $N = 3$ and systematically varied the curiosity weight α across a wide range (from 0.0 to 1.0) on the **Pascal VOC** dataset. We then observed its effect on the tail-performance metric, **Rare-F1**.

Results and Analyses. The results in Figure 3 show a clear inverted U-shaped curve for Rare-F1 as a function of α . When $\alpha = 0$ (i.e., no curiosity), Rare-F1 is the lowest, highlighting that the absence of explicit tail exploration leads to insufficient tail coverage. As α increases, Rare-F1 rises steadily and achieves its maximum within the range $\alpha \in [0.3, 0.6]$, indicating that a moderate curiosity strength most effectively steers the model toward rare-label discovery and specialization. However, as α continues to grow past 0.7, performance starts to decline. This drop suggests that overemphasis on tail exploration begins to hurt overall optimization—the model may overfit to rare labels or sacrifice global consistency, confirming the necessity of balance.

This pattern quantitatively demonstrates two key points: (1) the curiosity mechanism is indeed essential for robust tail performance, and (2) CD-GTMLL maintains robustness and stable gains across a wide, intuitive range of α . As such, our CD-GTMLL does not require brittle fine-tuning and is amenable to practical deployment.

4.8.2 Impact of Number of Players N .

Experimental Setup. We have fixed the other hyperparameters and varied the number of players N (from 1 to 8) on the **Pascal VOC** dataset. We observed the effect on both a head-centric metric (**mAP**) and a tail-centric metric (**Rare-F1**).

Results and Analyses. The results, corresponding to Figure 4, provide a nuanced view of the cost-benefit trade-off in the multi-player design, i.e., Significant Leap from $N=1$ to $N=3$. Both mAP and Rare-F1 see their largest increase when moving from a single predictor ($N = 1$) to a multi-player game ($N = 3$). Specifically, mAP rises from 90.1% to 92.7%, and Rare-F1 jumps from 75.1% to 79.2%. This demonstrates the intrinsic value of cooperative specialization and disagreement in capturing rare concepts. Performance Saturation: As N increases to 5 or 6, Rare-F1 continues to improve slightly (peaking at 80.5% for $N = 6$), but mAP remains stable, suggesting diminishing marginal returns as division of labor increases. Diminishing Returns and Overfitting: When $N > 6$, Rare-F1 and mAP both plateau or even decrease slightly. Excessive players lead to smaller, less representative label subsets and overfitting, while $N = 3$ to 5 achieves the optimal balance between tail performance, accuracy, and computational cost.

5 Conclusion

In this work, we introduced **Curiosity-Driven Game-Theoretic Multi-Label Learning (CD-GTMLL)**, a novel framework that re-conceptualizes long-tail multi-label classification as a cooperative game among specialized sub-predictors. By endowing each player with an intrinsic curiosity reward—scaled according to label rarity and inter-player disagreement—our method dynamically amplifies gradient signals for underrepresented classes without manual hyperparameter tuning. We provided a formal analysis demonstrating the existence of a tail-aware Nash equilibrium and established convergence guarantees that tie directly to improvements in the Rare-F1 metric. Our CD-GTMLL consistently outperforms state-of-the-art baselines across a diverse suite of benchmarks, including Pascal VOC, MS-COCO, Yeast, Mediamill, Eurlex-4K, Wiki10-31K, and AmazonCat-13K. Notably, under both standard and artificially intensified long-tail conditions, our approach achieves substantial gains in mAP, $P@k$, and Rare-F1, while maintaining only linear training overhead and negligible inference cost.

References

- [1] Ziad Abdallah, Ali El-Zaart, and Mohamad Oueidat. 2015. Comparison of multi-label problem transformation methods for text mining. In *2015 Fifth International Conference on Digital Information and Communication Technology and its Applications (DICTAP)*. 115–118. doi:10.1109/DICTAP.2015.7113182
- [2] Emanuel Ben-Baruch, Tal Ridnik, Nadav Zamir, Asaf Noy, Itamar Friedman, Matan Protter, and Lihi Zelnik-Manor. 2021. Asymmetric Loss For Multi-Label Classification. arXiv:2009.14119 [cs.CV] <https://arxiv.org/abs/2009.14119>
- [3] Matthew R Boutell, Jiebo Luo, Xiaotong Shen, and C Lee Brown. 2004. Learning multi-label scene classification. *Pattern Recognition* 37, 9 (2004), 1757–1771.

[4] Kaidi Cao, Colin Wei, Adrien Gaidon, Nikos Archiga, and Tengyu Ma. 2019. Learning Imbalanced Datasets with Label-Distribution-Aware Margin Loss. *arXiv:1906.07413 [cs.LG]* <https://arxiv.org/abs/1906.07413>

[5] Francisco Charte, Antonio J. Rivera, María José del Jesus, and Francisco Herrera. 2015. Addressing imbalance in multilabel classification: Measures and random resampling algorithms. *Neurocomputing* 163 (2015), 3–16. doi:10.1016/j.neucom.2014.08.091

[6] Lin Chen, Jingkuan Song, Xuerui Zhang, and Mingsheng Shang. 2022. MCFL: Multi-label Contrastive Focal Loss for Deep Imbalanced Pedestrian Attribute Recognition. *Neural Computing and Applications* 34, 18 (2022), 14357–14368. doi:10.1007/s00521-022-07300-7

[7] Yiyang Chen, Xuanhua He, Xiujun Ma, and Yue Ma. 2025. ContextFlow: Training-Free Video Object Editing via Adaptive Context Enrichment. *arXiv preprint arXiv:2509.17818* (2025).

[8] Zhao-Min Chen, Xiu-Shen Wei, Peng Wang, and Yanwen Guo. 2019. Multi-Label Image Recognition With Graph Convolutional Networks. In *2019 IEEE/CVF Conference on Computer Vision and Pattern Recognition (CVPR)*. 5172–5181. doi:10.1109/CVPR.2019.00532

[9] Arpan Dasgupta, Preeti Lamba, Ankita Kushwaha, Kiran Ravish, Siddhant Katyan, ShrutiDas, and Pawan Kumar. 2025. Review of Extreme Multilabel Classification. *arXiv:2302.05971 [cs.LG]* <https://arxiv.org/abs/2302.05971>

[10] Krzysztof Dembczynski, Weiwei Cheng, and Eyke Hüllermeier. 2010. Bayes optimal multilabel classification via probabilistic classifier chains. In *Proceedings of the 27th International Conference on International Conference on Machine Learning (Haifa, Israel) (ICML'10)*. Omnipress, Madison, WI, USA, 279–286.

[11] Lih Dery. 2023. *Multi-Label Ranking: Mining Multi-Label and Label Ranking Data*. Springer International Publishing, 511–535. doi:10.1007/978-3-031-24628-9_23

[12] André Elisseeff and Jason Weston. 2001. A kernel method for multi-labelled classification. In *Advances in Neural Information Processing Systems*, Vol. 14. 681–687. https://papers.nips.cc/paper_files/paper/2001/hash/39dcfa0a53dc372fb391d4e6b5d693-Abstract.html

[13] M. Everingham, L. Van Gool, C. K. I. Williams, J. Winn, and A. Zisserman. [n. d.]. The PASCAL Visual Object Classes Challenge 2007 (VOC2007) Results. <http://www.pascal-network.org/challenges/VOC/voc2007/workshop/index.html>

[14] Yuling Fan, Jinghua Liu, Jianeng Tang, Peizhong Liu, Y. Lin, and Y. Du. 2024. Learning correlation information for multi-label feature selection. *Pattern Recognition* 145 (2024), 109899. doi:10.1016/j.patcog.2023.109899

[15] Yijia Fan, Jusheng Zhang, Kaitong Cai, Jing Yang, Chengpei Tang, Jian Wang, and Keze Wang. 2025. Cost-Effective Communication: An Auction-based Method for Language Agent Interaction. *arXiv:2511.13193 [cs.AI]* <https://arxiv.org/abs/2511.13193>

[16] Yijia Fan, Jusheng Zhang, Kaitong Cai, Jing Yang, and Keze Wang. 2025. CCG: Rare-Label Prediction via Neural SEM-Driven Causal Game. In *Findings of the Association for Computational Linguistics: EMNLP 2025*. Christos Christodoulopoulos, Tanmoy Chakraborty, Carolyn Rose, and Violet Peng (Eds.). Association for Computational Linguistics, Suzhou, China, 6243–6256. doi:10.18653/v1/2025.findings-emnlp.331

[17] Yi Huang, Buse Giledereli, Abdullatif Köksal, Arzucan Özgür, and Elif Ozkirimi. 2021. Balancing Methods for Multi-label Text Classification with Long-Tailed Class Distribution. *arXiv:2109.04712 [cs.CL]* <https://arxiv.org/abs/2109.04712>

[18] Himanshu Jain. 2018. Extreme Classification - URELex. <https://kaggle.com/competitions/extreme-classification-urelex>. Kaggle.

[19] Wojciech Kotłowski and Krzysztof Dembczynski. 2016. Surrogate regret bounds for generalized classification performance metrics. *arXiv:1504.07272 [cs.LG]* <https://arxiv.org/abs/1504.07272>

[20] Oluwaseun O. Koyejo, Nagarajan Natarajan, Pradeep K. Ravikumar, and Inderjit S. Dhillon. 2015. Consistent Multi-label Classification. In *Advances in Neural Information Processing Systems*, Vol. 28. 3321–3329. <https://proceedings.neurips.cc/paper/2015/file/85f007f8c50dd25f5a45fea73cad64bd-Paper.pdf>

[21] Jack Lanchantin, Tianli Wang, Vicente Ordonez, and Yanjun Qi. 2021. General Multi-label Image Classification with Transformers. In *2021 IEEE/CVF Conference on Computer Vision and Pattern Recognition (CVPR)*. 16473–16483. doi:10.1109/CVPR46437.2021.01621

[22] Weiqi Li, Fan Lyu, Fahuan Shang, Liang Wan, and Wei Feng. 2023. Long-Tailed Learning as Multi-Objective Optimization. *arXiv:2310.20490 [cs.CV]* <https://arxiv.org/abs/2310.20490>

[23] Xiaohua Li, Jusheng Zhang, and Fatemeh Safara. 2021. Improving the Accuracy of Diabetes Diagnosis Applications through a Hybrid Feature Selection Algorithm. *Neural Process. Lett.* 55, 1 (March 2021), 153–169. doi:10.1007/s11063-021-10491-0

[24] Tsung-Yi Lin, Michael Maire, Serge Belongie, Lubomir Bourdev, Ross Girshick, James Hays, Pietro Perona, Deva Ramanan, C. Lawrence Zitnick, and Piotr Dollar. 2015. Microsoft COCO: Common Objects in Context. *arXiv:1405.0312 [cs.CV]* <https://arxiv.org/abs/1405.0312>

[25] Yang Liu, Keze Wang, Lingbo Liu, Haoyuan Lan, and Liang Lin. 2022. TCGL: Temporal Contrastive Graph for Self-Supervised Video Representation Learning. *IEEE Transactions on Image Processing* 31 (2022), 1978–1993. doi:10.1109/TIP.2022.3147032

[26] Yue Ma, Hongyu Liu, Hongfa Wang, Heng Pan, Yingqing He, Junkun Yuan, Ailing Zeng, Chengfei Cai, Heung-Yeung Shum, Wei Liu, et al. 2024. Follow-your-emoji: Fine-controllable and expressive freestyle portrait animation. In *SIGGRAPH Asia 2024 Conference Papers*. 1–12.

[27] Yue Ma, Yulong Liu, Qiyuan Zhu, Ayden Yang, Kunyu Feng, Xinhua Zhang, Zhiheng Li, Sirui Han, Chenyang Qi, and Qifeng Chen. 2025. Follow-Your-Motion: Video Motion Transfer via Efficient Spatial-Temporal Decoupled Finetuning. *arXiv preprint arXiv:2506.05207* (2025).

[28] Yue Ma, Zexuan Yan, Hongyu Liu, Hongfa Wang, Heng Pan, Yingqing He, Junkun Yuan, Ailing Zeng, Chengfei Cai, Heung-Yeung Shum, et al. 2025. Follow-your-emoji-faster: Towards efficient, fine-controllable, and expressive freestyle portrait animation. *arXiv preprint arXiv:2509.16630* (2025).

[29] Sean MacAvaney, Franck Dernoncourt, Walter Chang, Nazli Goharian, and Ophir Frieder. 2020. Interaction Matching for Long-Tail Multi-Label Classification. *arXiv:2005.08805 [cs.CL]* <https://arxiv.org/abs/2005.08805>

[30] Amirreza Mahdavi-Shahri, Mahboobeh Houshmand, Mahdi Yaghoobi, and Mehrdad Jalali. 2016. Applying an ensemble learning method for improving multi-label classification performance. In *2016 2nd International Conference of Signal Processing and Intelligent Systems (ICSPIS)*. IEEE, 1–6. doi:10.1109/icspis.2016.7869900

[31] Julian McAuley and Jure Leskovec. 2013. Hidden factors and hidden topics: understanding rating dimensions with review text. In *Proceedings of the 7th ACM Conference on Recommender Systems (Hong Kong, China) (RecSys '13)*. Association for Computing Machinery, New York, NY, USA, 165–172. doi:10.1145/2507157.2507163

[32] Deepak Pathak, Pulkit Agrawal, Alexei A. Efros, and Trevor Darrell. 2017. Curiosity-driven Exploration by Self-supervised Prediction. *arXiv:1705.05363 [cs.LG]* <https://arxiv.org/abs/1705.05363>

[33] Jesse Read, Bernhard Pfahringer, Geoff Holmes, and Eibe Frank. 2008. Pruned Problem Transformation Methods for Multi-label Classification. In *European Conference on Machine Learning and Principles and Practice of Knowledge Discovery in Databases (ECML-PKDD)*. 143–147.

[34] Jesse Read, Bernhard Pfahringer, Geoff Holmes, and Eibe Frank. 2009. Classifier Chains for Multi-Label Classification. *Lecture Notes in Computer Science*, Vol. 5783. Springer, 254–269. https://link.springer.com/chapter/10.1007/978-3-642-04174-7_17

[35] Jesse Read, Bernhard Pfahringer, Geoffrey Holmes, and Eibe Frank. 2021. Classifier Chains: A Review and Perspectives. *Journal of Artificial Intelligence Research* 70 (Feb. 2021), 683–718. doi:10.1613/jair.1.12376

[36] Tal Ridnik, Gilad Sharir, Avi Ben-Cohen, Emanuel Ben-Baruch, and Asaf Noy. 2023. ML-Decoder: Scalable and Versatile Classification Head. In *2023 IEEE/CVF Winter Conference on Applications of Computer Vision (WACV)*. 32–41. doi:10.1109/WACV56688.2023.00012

[37] Cees G. M. Snoek, Marcel Worring, Jan C. van Gemert, Jan-Mark Geusebroek, and Arnold W. M. Smeulders. 2006. The challenge problem for automated detection of 101 semantic concepts in multimedia. In *Proceedings of the 14th ACM International Conference on Multimedia (Santa Barbara, CA, USA) (MM '06)*. Association for Computing Machinery, New York, NY, USA, 421–430. doi:10.1145/1180639.1180727

[38] Hwanjun Song, Minseok Kim, and Jae Gil Lee. 2024. Toward Robustness in Multi-Label Classification: A Data Augmentation Strategy against Imbalance and Noise. In *Proceedings of the AAAI Conference on Artificial Intelligence*, Vol. 38. 21592–21601. doi:10.1609/aaai.v38i19.30157

[39] Peter Sunehag, Guy Lever, Audrunas Gruslys, Wojciech Marian Czarnecki, Vincenzo Zambaldi, Max Jaderberg, Marc Lanctot, Nicolas Sonnerat, Joel Z. Leibo, Karl Tuyls, and Thore Graepel. 2017. Value-Decomposition Networks For Cooperative Multi-Agent Learning. *arXiv:1706.05296 [cs.AI]* <https://arxiv.org/abs/1706.05296>

[40] Zijian Tao, Shao-Yuan Li, Wenhui Wan, Jinpeng Zheng, Jia-Yao Chen, Yuchen Li, Sheng-Jun Huang, and Songcan Chen. 2025. MLC-NC: Long-Tailed Multi-Label Image Classification Through the Lens of Neural Collapse. In *Proceedings of the AAAI Conference on Artificial Intelligence*, Vol. 39. 1234–1242. doi:10.1609/aaai.v39i1.34298

[41] Adane Nega Tarekegn, Mohib Ullah, and Faouzi Alaya Cheikh. 2024. Deep Learning for Multi-Label Learning: A Comprehensive Survey. *arXiv:2401.16549 [cs.LG]* <https://arxiv.org/abs/2401.16549>

[42] Zeyu Teng, Peng Cao, Min Huang, Zheming Gao, and Xingwei Wang. 2024. Multi-label Borderline Oversampling Technique. *Pattern Recognition* 145 (2024), 109953. doi:10.1016/j.patcog.2023.109953

[43] Ermal Toto, ML Tlachac, and Elke A. Rundensteiner. 2021. AudiBERT: A Deep Transfer Learning Multimodal Classification Framework for Depression Screening. In *Proceedings of the 30th ACM International Conference on Information & Knowledge Management (Virtual Event, Queensland, Australia) (CIKM '21)*. Association for Computing Machinery, New York, NY, USA, 4145–4154. doi:10.1145/3459637.3481895

[44] Guangrun Wang, Keze Wang, Guangcong Wang, Philip H.S. Torr, and Liang Lin. 2021. Solving Inefficiency of Self-Supervised Representation Learning. In *Proceedings of the IEEE/CVF International Conference on Computer Vision (ICCV)*. 9505–9515.

[45] Keze Wang, Dongyu Zhang, Ya Li, Ruimao Zhang, and Liang Lin. 2017. Cost-Effective Active Learning for Deep Image Classification. *IEEE Transactions on Circuits and Systems for Video Technology* 27, 12 (2017), 2591–2600. doi:10.1109/TCST.2016.2589879

[46] Tong Wei, Zhen Mao, Jiang-Xin Shi, Yu-Feng Li, and Min-Ling Zhang. 2022. A Survey on Extreme Multi-label Learning. arXiv:2210.03968 [cs.LG] <https://arxiv.org/abs/2210.03968>

[47] Wei Weng, Da-Han Wang, Chin-Ling Chen, Juan Wen, and Shun-Xiang Wu. 2020. Label Specific Features-Based Classifier Chains for Multi-Label Classification. *IEEE Access* 8 (2020), 51265–51275. doi:10.1109/ACCESS.2020.2980551

[48] Tong Wu, Qingguo Huang, Ziwei Liu, Yu Wang, and Dahu Lin. 2021. Distribution-Balanced Loss for Multi-Label Classification in Long-Tailed Datasets. arXiv:2007.09654 [cs.CV] <https://arxiv.org/abs/2007.09654>

[49] Pengyu Xu, Lin Xiao, Bing Liu, Sijin Lu, Liping Jing, and Jian Yu. 2023. Label-specific feature augmentation for long-tailed multi-label text classification. In *Proceedings of the Thirty-Seventh AAAI Conference on Artificial Intelligence and Thirty-Fifth Conference on Innovative Applications of Artificial Intelligence and Thirteenth Symposium on Educational Advances in Artificial Intelligence (AAAI'23/IAAI'23/EEAI'23)*. AAAI Press, Article 1190, 9 pages. doi:10.1609/aaai.v37i9.26259

[50] Yan Yan, Junyuan Liu, and Bo-Wen Zhang. 2025. LabelCoRank: Revolutionizing Long Tail Multi-Label Classification with Co-Occurrence Reranking. arXiv:2503.07968 [cs.CL] <https://arxiv.org/abs/2503.07968>

[51] Pengcheng Yang, Xu Sun, Wei Li, Shuming Ma, Wei Wu, and Houfeng Wang. 2018. SGM: Sequence Generation Model for Multi-label Classification. arXiv:1806.04822 [cs.CL] <https://arxiv.org/abs/1806.04822>

[52] Jiawei Yao, Jusheng Zhang, Xiaochao Pan, Tong Wu, and Canran Xiao. 2024. DepthSSC: Monocular 3D Semantic Scene Completion via Depth-Spatial Alignment and Voxel Adaptation. arXiv:2311.17084 [cs.CV] <https://arxiv.org/abs/2311.17084>

[53] Hui Ye, Rajshekhar Sunderraman, and Shihao Ji. 2024. MatchXML: An Efficient Text-label Matching Framework for Extreme Multi-label Text Classification. arXiv:2308.13139 [cs.CL] <https://arxiv.org/abs/2308.13139>

[54] Mengqi Yuan, Jinke Xu, and Zhongnian Li. 2019. Long Tail Multi-label Learning. In *2019 IEEE Second International Conference on Artificial Intelligence and Knowledge Engineering (AIKE)*. 28–31. doi:10.1109/AIKE.2019.00013

[55] Jusheng Zhang, Kaitong Cai, Yijia Fan, Ningyuan Liu, and Keze Wang. 2025. MAT-Agent: Adaptive Multi-Agent Training Optimization. In *The Thirty-ninth Annual Conference on Neural Information Processing Systems*. <https://openreview.net/forum?id=YDWRTYgR79>

[56] Jusheng Zhang, Kaitong Cai, Yijia Fan, Jian Wang, and Keze Wang. 2025. CF-VLM: Counterfactual Vision-Language Fine-tuning. In *The Thirty-ninth Annual Conference on Neural Information Processing Systems*. <https://openreview.net/forum?id=0qGtaRTsCo>

[57] Jusheng Zhang, Kaitong Cai, Xiaoyang Guo, Sidi Liu, Qinhan Lv, Ruiqi Chen, Jing Yang, Yijia Fan, Xiaofei Sun, Jian Wang, Ziliang Chen, Liang Lin, and Keze Wang. 2025. MM-CoT: A Benchmark for Probing Visual Chain-of-Thought Reasoning in Multimodal Models. arXiv:2512.08228 [cs.CV] <https://arxiv.org/abs/2512.08228>

[58] Jusheng Zhang, Kaitong Cai, Jian Wang, Yongsen Zheng, Kwok-Yan Lam, and Keze Wang. 2026. Process-of-Thought Reasoning for Videos. arXiv:2602.07689 [cs.CV] <https://arxiv.org/abs/2602.07689>

[59] Jusheng Zhang, Kaitong Cai, Jing Yang, Jian Wang, Chengpei Tang, and Keze Wang. 2025. Top-Down Semantic Refinement for Image Captioning. arXiv:2510.22391 [cs.CV] <https://arxiv.org/abs/2510.22391>

[60] Jusheng Zhang, Kaitong Cai, Jing Yang, and Keze Wang. 2025. Learning Dynamics of VLM Finetuning. arXiv:2510.11978 [cs.LG] <https://arxiv.org/abs/2510.11978>

[61] Jusheng Zhang, Kaitong Cai, Qinglin Zeng, Ningyuan Liu, Stephen Fan, Ziliang Chen, and Keze Wang. 2025. Failure-Driven Workflow Refinement. arXiv:2510.10035 [cs.AI] <https://arxiv.org/abs/2510.10035>

[62] Jiong Zhang, Wei cheng Chang, Hsiang fu Yu, and Inderjit S. Dhillon. 2021. Fast Multi-Resolution Transformer Fine-tuning for Extreme Multi-label Text Classification. arXiv:2110.00685 [cs.LG] <https://arxiv.org/abs/2110.00685>

[63] Jusheng Zhang, Yijia Fan, Kaitong Cai, Zimeng Huang, Xiaofei Sun, Jian Wang, Chengpei Tang, and Keze Wang. 2025. DrDiff: Dynamic Routing Diffusion with Hierarchical Attention for Breaking the Efficiency-Quality Trade-off. arXiv:2509.02785 [cs.CL] <https://arxiv.org/abs/2509.02785>

[64] Jusheng Zhang, Yijia Fan, Kaitong Cai, Xiaofei Sun, and Keze Wang. 2025. OSC: Cognitive Orchestration through Dynamic Knowledge Alignment in Multi-Agent LLM Collaboration. arXiv:2509.04876 [cs.AI] <https://arxiv.org/abs/2509.04876>

[65] Jusheng Zhang, Yijia Fan, Kaitong Cai, and Keze Wang. 2025. Kolmogorov-Arnold Fourier Networks. arXiv:2502.06018 [cs.LG] <https://arxiv.org/abs/2502.06018>

[66] Jusheng Zhang, Yijia Fan, Kaitong Cai, Jing Yang, Jiawei Yao, Jian Wang, Guanlong Qu, Ziliang Chen, and Keze Wang. 2026. Why Keep Your Doubts to Yourself? Trading Visual Uncertainties in Multi-Agent Bandit Systems. arXiv:2601.18735 [cs.AI] <https://arxiv.org/abs/2601.18735>

[67] Jusheng Zhang, Yijia Fan, Kaitong Cai, Jing Yang, Yongsen Zheng, Kwok-Yan Lam, Liang Lin, and Keze Wang. 2026. Spectral Gating Networks. arXiv:2602.07679 [cs.LG] <https://arxiv.org/abs/2602.07679>

[68] Jusheng Zhang, Yijia Fan, Wenjun Lin, Ruiqi Chen, Haoyi Jiang, Wenhao Chai, Jian Wang, and Keze Wang. 2025. GAM-Agent: Game-Theoretic and Uncertainty-Aware Collaboration for Complex Visual Reasoning. In *The Thirty-ninth Annual Conference on Neural Information Processing Systems*. <https://openreview.net/forum?id=EKJhU5ioSo>

[69] Jusheng Zhang, Yijia Fan, Zimo Wen, Jian Wang, and Keze Wang. 2025. Tri-MARF: A Tri-Modal Multi-Agent Responsive Framework for Comprehensive 3D Object Annotation. In *The Thirty-ninth Annual Conference on Neural Information Processing Systems*. <https://openreview.net/forum?id=YGlbwfNWot>

[70] Jusheng Zhang, Xiaoyang Guo, Kaitong Cai, Qinhan Lv, Yijia Fan, Wenhao Chai, Jian Wang, and Keze Wang. 2025. HybridToken-VLM: Hybrid Token Compression for Vision-Language Models. arXiv:2512.08240 [cs.CV] <https://arxiv.org/abs/2512.08240>

[71] Jusheng Zhang, Zimeng Huang, Yijia Fan, Ningyuan Liu, Mingyan Li, Zhuojie Yang, Jiawei Yao, Jian Wang, and Keze Wang. 2025. KABB: Knowledge-Aware Bayesian Bandits for Dynamic Expert Coordination in Multi-Agent Systems. In *Forty-second International Conference on Machine Learning*. <https://openreview.net/forum?id=AKV9a4jho>

[72] Jensen Zhang, Ningyuan Liu, Yijia Fan, Zihao Huang, Qinglin Zeng, Kaitong Cai, Jian Wang, and Keze Wang. 2025. LLM-CAS: Dynamic Neuron Perturbation for Real-Time Hallucination Correction. arXiv:2512.18623 [cs.CL] <https://arxiv.org/abs/2512.18623>

[73] Jusheng Zhang, Ningyuan Liu, Qinhan Lyu, Jing Yang, and Keze Wang. 2026. Rational ANOVA Networks. arXiv:2602.04006 [cs.LG] <https://arxiv.org/abs/2602.04006>

[74] Min-Ling Zhang and Zhi-Hua Zhou. 2014. A Review on Multi-Label Learning Algorithms. *IEEE Transactions on Knowledge and Data Engineering* 26, 8 (2014), 1819–1837. doi:10.1109/TKDE.2013.39

[75] Xingyu Zhao, Yuxuan An, Ning Xu, Jing Wang, and Xiang Geng. 2023. Imbalanced Label Distribution Learning. In *Proceedings of the Thirty-Seventh AAAI Conference on Artificial Intelligence (AAAI)*, Vol. 37. 11336–11344. doi:10.1609/aaai.v37i9.26341

[76] Xiaoqiang Zheng, Zhenxia Yu, Lin Chen, Fan Zhu, and Shilong Wang. 2021. Multi-label Contrastive Focal Loss for Pedestrian Attribute Recognition. In *2020 25th International Conference on Pattern Recognition (ICPR)*. 7349–7356. doi:10.1109/ICPR48806.2021.9411959

[77] Ke Zhu, Minghao Fu, and Jianxin Wu. 2023. Multi-Label Self-Supervised Learning with Scene Images. arXiv:2308.03286 [cs.CV] <https://arxiv.org/abs/2308.03286>

[78] Arkaitz Zubiaga. 2012. *Enhancing Navigation on Wikipedia with Social Tags*. arXiv:1202.5469 [cs.IR] <https://arxiv.org/abs/1202.5469>

A Theoretical Proofs

This section provides the detailed mathematical derivations that underpin the theoretical claims of our CD-GTMLL framework. We first present the complete proof for the existence of a tail-aware Nash equilibrium and then formally establish the connection between our optimization objective and the Rare-F1 metric[26–28].

A.1 Proof of Theorem 1 (Existence of a Tail-Aware Equilibrium)

We begin by restating the theorem and the core assumptions from the main manuscript for clarity. The following conditions hold: (i) Each player's parameter set Θ_i is a non-empty, compact, and convex subset of a Euclidean space. (ii) The shared cooperative payoff function $R(\{\theta_i\}_{i=1}^N)$ is continuous on the joint parameter space $\Theta = \prod_{i=1}^N \Theta_i$. (iii) The performance metric \mathcal{M} is tail-responsive, meaning any improvement in accuracy on a tail label results in a non-negative change in \mathcal{M} .

Theorem 2. Under Assumption 1, there exists a global maximizer $(\theta_1^*, \dots, \theta_N^*) \in \prod_i \Theta_i$ of the cooperative objective. Every such maximizer is a pure-strategy Nash equilibrium, and no such equilibrium can systematically ignore all tail labels.

PROOF. The proof proceeds in three stages: (1) establishing the existence of a global maximizer, (2) showing that this maximizer constitutes a pure-strategy Nash Equilibrium, and (3) arguing that the equilibrium is necessarily tail-aware.

1. Existence of a Global Maximizer.

Let the joint parameter space for all N players be $\Theta = \prod_{i=1}^N \Theta_i$. According to Assumption 1(i), each Θ_i is non-empty and compact. By Tychonoff's theorem, the product of a finite number of compact sets is itself compact. Therefore, the joint parameter space Θ is non-empty and compact.

The game is defined as a cooperative game where all players optimize a shared objective. We can define a global potential function $\Phi : \Theta \rightarrow \mathbb{R}$ that all players implicitly maximize

$$\Phi(\theta) = R(\theta) + \alpha \sum_{i=1}^N \mathbb{E}_{x \sim \mathcal{D}} [C_i(x; \theta)]$$

, where $\theta = \{\theta_i\}_{i=1}^N$, $R(\theta)$ is the global payoff, and $C_i(x; \theta)$ is the curiosity reward for player i as defined in Equation (5) of the main text.

Per Assumption 1(ii), $R(\theta)$ is continuous on Θ . The curiosity term $C_i(x; \theta)$ is composed of indicator functions and a KL divergence term, which are continuous functions of the network outputs $\pi_i(x; \theta_i)$. As neural networks with standard activations are continuous functions of their parameters θ_i , the entire curiosity term $\mathbb{E}_x [C_i(x; \theta)]$ is continuous with respect to θ . The sum of continuous functions is continuous, so the potential function $\Phi(\theta)$ is continuous on the compact set Θ .

By the Weierstrass Extreme Value Theorem, a continuous function on a non-empty, compact set must attain a maximum value. Therefore, there exists at least one global maximizer $\theta^* = (\theta_1^*, \dots, \theta_N^*) \in \Theta$ such that $\Phi(\theta^*) \geq \Phi(\theta)$ for all $\theta \in \Theta$.

2. The Global Maximizer is a Nash Equilibrium.

A parameter profile θ^* is a pure-strategy Nash Equilibrium if, for every player i , no player can improve its individual payoff by

unilaterally deviating from its strategy θ_i^* . The payoff for player i is $J_i(\theta) = R(\theta) + \alpha \mathbb{E}_x [C_i(x; \theta)]$.

Consider the global maximizer θ^* . By definition, for any player k and any alternative strategy $\theta'_k \in \Theta_k$:

$$\Phi(\theta_1^*, \dots, \theta_k^*, \dots, \theta_N^*) \geq \Phi(\theta_1^*, \dots, \theta'_k, \dots, \theta_N^*)$$

This is a potential game where the change in the potential function equals the change in the deviating player's utility function. Thus, for player k , deviating from θ_k^* to θ'_k does not increase their individual payoff J_k . This holds for all players $k = 1, \dots, N$. Therefore, θ^* is a pure-strategy Nash Equilibrium.

3. The Equilibrium is Tail-Aware.

The equilibrium is "tail-aware" because systematically ignoring tail labels is not a stable strategy. According to Proposition 1 from the main text, if a parameter profile misclassifies a tail label for which the model has sufficient capacity to learn, the gradient $\nabla_{\theta_k} J_k$ for the responsible player k is strictly positive in the direction that corrects the error. At an equilibrium θ^* , the conditions for optimality imply that for players updated with gradient ascent, the gradient must be zero. A state where tail labels are systematically ignored while head labels are correctly classified would produce a non-zero gradient from the curiosity term C_i , pushing the parameters away from that state. Furthermore, because the global metric \mathcal{M} is tail-responsive (Assumption 1(iii)), any improvement on tail labels does not harm the global objective, ensuring that players are not penalized for learning them. Thus, any equilibrium found must have addressed the tail labels to the best of the model's capacity. \square

A.2 Formal Link between Optimization Objective and Rare-F1

We now formally demonstrate that maximizing our proposed objective function inherently promotes the improvement of the Rare-F1 score, which is a key metric for evaluating performance on the tail distribution.

Definition 3 (Rare-F1). The Rare-F1 score is the F1-score computed exclusively on the set of tail labels, \mathcal{L}_T . It is the harmonic mean of tail precision (P_T) and tail recall (R_T):

$$\text{Rare-F1} = \frac{2 \cdot P_T \cdot R_T}{P_T + R_T}, \quad \text{where } R_T = \frac{TP_T}{TP_T + FN_T}$$

Here, TP_T and FN_T are the number of true positives and false negatives on the tail label set \mathcal{L}_T , respectively.

Proposition 2. Maximizing the CD-GTMLL objective function, $J(\theta) = \sum_i J_i(\theta)$, implies the maximization of a weighted form of tail-set recall, thereby directly optimizing for a component of the Rare-F1 score.

PROOF. The total objective across all players can be written as:

$$J(\theta) = N \cdot R(\theta) + \alpha \sum_{i=1}^N \mathbb{E}_x [C_i(x; \theta)]$$

Let us isolate the component of the curiosity reward that directly pertains to correct classifications on the tail set \mathcal{L}_T . This component, which we denote C^{tail} , is:

$$C^{\text{tail}}(x, y, \theta) = \sum_{i=1}^N \sum_{l \in \mathcal{L}_i \cap \mathcal{L}_T} \frac{\mathbb{I}(\hat{y}_l = y_l)}{1 + freq(l)}$$

where $\mathbb{I}(\cdot)$ is the indicator function and \hat{y}_l is the final prediction for label l .

The term $\mathbb{I}(\hat{y}_l = y_l)$ can be expanded into true positives and true negatives. For improving recall, we are interested in true positives, where $y_l = 1$ and $\hat{y}_l = 1$. Let's analyze the contribution to the objective from a single positive instance (x, y) where $y_l = 1$ for some $l \in \mathcal{L}_T$. A correct prediction ($\hat{y}_l = 1$) contributes $\frac{1}{1+freq(l)}$ to the curiosity term for each player responsible for label l . An incorrect prediction ($\hat{y}_l = 0$) contributes 0.

Therefore, maximizing the expectation of C^{tail} over the data distribution \mathcal{D} is equivalent to maximizing:

$$\mathbb{E}_{(x,y) \sim \mathcal{D}} \left[\sum_{l \in \mathcal{L}_T} w_l \cdot \mathbb{I}(\hat{y}_l = 1 \text{ and } y_l = 1) \right]$$

where $w_l = \frac{|\{i: l \in \mathcal{L}_i\}|}{1+freq(l)}$ is a large positive weight for infrequent labels. This expectation is a weighted sum of probabilities of true positive predictions across all tail labels. Maximizing this is equivalent to maximizing the weighted number of true positives on the tail set, $\sum_{l \in \mathcal{L}_T} w_l \text{TP}_l$.

Since tail recall R_T is a monotonically increasing function of the number of true positives TP_T , and our objective function contains a term that is a strongly weighted sum of tail-set true positives, the optimization process is directly incentivized to increase R_T . An increase in R_T , holding P_T constant or also improving it, leads to an increase in the Rare-F1 score.

Thus, our framework does not merely hope for better tail performance as a side effect; it embeds a surrogate for tail-set recall directly into its objective function, formally linking the optimization dynamics to improvement in the Rare-F1 metric. \square

A.3 Pseudocode for Label Set Partitioning

To enforce a structured division of labor among players, the total label set \mathcal{L} is partitioned based on label frequency. The following procedure guarantees a systematic and reproducible allocation of overlapping label subsets to each of the N players, promoting specialization while maintaining informational redundancy at partition boundaries. The degree of redundancy is controlled by the overlap ratio hyperparameter, ρ .

A.4 Implementation of Fusion Strategies

The global fusion operator $g(\{\pi_i(x; \theta_i)\}_{i=1}^N)$ is a critical component for aggregating predictions from specialized players into a single, coherent output vector $\hat{p} \in [0, 1]^L$. The choice of operator dictates the nature of inter-player collaboration. While the main paper utilizes a weighted average, several alternative differentiable strategies exist, each with distinct operational trade-offs.

Weighted Averaging (Baseline). As defined in Equation (3) of the main manuscript, this strategy computes the fused prediction for a label l as a weighted average of outputs from all players responsible for it:

$$\hat{p}_l = \sum_{i: l \in \mathcal{L}_i} \omega_{i,l} [\pi_i(x; \theta_i)]_l, \quad \text{with} \quad \sum_{i: l \in \mathcal{L}_i} \omega_{i,l} = 1$$

The weights $\omega_{i,l}$ can be static (e.g., inversely proportional to the rank of the player's primary label block) or uniform (see Simple

Algorithm 2 Frequency-Based Overlapping Label Partitioning

```

1: Input: Full label set  $\mathcal{L}$  (where  $|\mathcal{L}| = L$ ), number of players  $N$ , overlap ratio  $\rho \in [0, 1]$ .
2: Data Requirement: Pre-computed frequency  $freq(l)$  for each label  $l \in \mathcal{L}$ .
3: Output: A list of  $N$  label subsets  $\{\mathcal{L}_1, \mathcal{L}_2, \dots, \mathcal{L}_N\}$ .
4: Let  $\mathcal{L}_{\text{sorted}} \leftarrow \text{Sort}(\mathcal{L}, \text{key} = freq, \text{descending} = \text{True})$ 
5: Let  $S \leftarrow \text{floor}(L/N)$   $\triangleright$  Calculate base size of each partition
6: Let  $O \leftarrow \text{floor}(S \times \rho/2)$   $\triangleright$  Calculate one-sided overlap size
7: for  $i = 1 \rightarrow N$  do
8:    $start\_index \leftarrow (i - 1) \times S$ 
9:    $end\_index \leftarrow i \times S - 1$ 
    $\triangleright$  Define core (non-overlapping) block for player  $i$ 
10:   $\mathcal{L}_{\text{core}} \leftarrow \mathcal{L}_{\text{sorted}}[start\_index : end\_index + 1]$ 
    $\triangleright$  Define overlapping regions with adjacent players
11:   $overlap\_prev\_start \leftarrow \max(0, start\_index - O)$ 
12:   $\mathcal{L}_{\text{overlap\_prev}} \leftarrow \mathcal{L}_{\text{sorted}}[overlap\_prev\_start : start\_index]$ 
13:   $overlap\_next\_end \leftarrow \min(L, end\_index + 1 + O)$ 
14:   $\mathcal{L}_{\text{overlap\_next}} \leftarrow \mathcal{L}_{\text{sorted}}[end\_index + 1 : overlap\_next\_end]$ 
    $\triangleright$  Construct final label set for player  $i$ 
15:   $\mathcal{L}_i \leftarrow \mathcal{L}_{\text{core}} \cup \mathcal{L}_{\text{overlap\_prev}} \cup \mathcal{L}_{\text{overlap\_next}}$ 
16: end for
17: return  $\{\mathcal{L}_1, \mathcal{L}_2, \dots, \mathcal{L}_N\}$ 

```

Averaging). This approach is robust and stable but may not fully leverage context-specific player expertise.

Max Pooling. This strategy operates under the assumption that for any given label, one player will develop superior expertise. The fusion is performed by selecting the most confident prediction among all relevant players:

$$\hat{p}_l = \max_{i: l \in \mathcal{L}_i} \{[\pi_i(x; \theta_i)]_l\}$$

This operator is computationally efficient and can yield decisive predictions if player specialization is pronounced. However, it is sensitive to overconfident errors from a single player and may lack the smoothing effect of averaging, potentially leading to higher variance in predictions.

Attention-based Fusion. A more dynamic and powerful approach is to learn the fusion weights contextually for each input instance x . A small attention module, parameterized by ϕ , can be trained to generate player- and label-specific weights:

$$\omega_{i,l}(x) = \text{softmax}_i(f_\phi(e(x), i, l))$$

Here, $e(x)$ is a shared feature embedding of the input x , and f_ϕ is a small neural network (e.g., a multi-layer perceptron) that scores the relevance of player i for label l given the input context. The final prediction is then a contextually weighted average:

$$\hat{p}_l = \sum_{i: l \in \mathcal{L}_i} \omega_{i,l}(x) [\pi_i(x; \theta_i)]_l$$

This method offers maximum flexibility, allowing the system to dynamically trust different players based on input features. The primary trade-off is increased model complexity and computational overhead during both training and inference, as the attention weights must be computed for each instance.

B Additional Hyperparameter Analyses

To provide a comprehensive operational profile of the CD-GTMLL framework and offer practical guidance for its deployment, we analyze the framework's sensitivity to two crucial hyperparameters that govern the nature of inter-player dynamics: the disagreement weight β and the label set overlap ratio ρ . All experiments in this section are conducted on the Pascal VOC 2007 dataset.

B.1 Impact of Disagreement Weight β

The hyperparameter β in the curiosity reward function balances the intrinsic reward between achieving correctness on rare labels and disagreeing with peer predictions. This disagreement term is the primary mechanism that drives structured exploration and prevents players from collapsing to a homogeneous consensus too early.

Evaluation Metric. To isolate the effect of β , we fixed the number of players to $N = 3$ and set the main curiosity weight to its optimal value ($\alpha = 0.5$). We then varied β across the range $[0.0, 0.05, 0.1, 0.2, 0.5, 1.0]$ and recorded the resulting mean Average Precision (mAP) and Rare-F1 scores.

Results and Analyses. The results, presented in Table 1, demonstrate that the disagreement mechanism is a vital component for robust tail-label performance. When $\beta = 0$, the exploration signal is purely based on static label rarity, resulting in suboptimal Rare-F1. As β increases, performance on tail labels rises significantly, peaking at $\beta = 0.2$. This indicates that a moderate incentive for disagreement effectively forces players to explore diverse predictive hypotheses for challenging instances, thereby improving collective performance on the tail. For excessively large β values, a marginal decline in both mAP and Rare-F1 is observed, as an overwhelming focus on inter-player disagreement can detract from the primary cooperative objective. The framework exhibits stable and strong performance across a wide range of β , confirming its tuning is not brittle.

Table 4: Sensitivity Analyses on the disagreement weight β on Pascal VOC 2007. Results are reported as mean \pm std over 3 runs. Best performance is in bold.

Disagreement Weight (β)	mAP (%)	Rare-F1 (%)
0.0	92.0 ± 0.4	76.5 ± 0.5
0.05	92.4 ± 0.3	78.1 ± 0.4
0.1	92.5 ± 0.3	78.9 ± 0.4
0.2	92.6 ± 0.2	79.3 ± 0.3
0.5	92.4 ± 0.3	79.0 ± 0.4
1.0	92.1 ± 0.4	78.6 ± 0.4

B.2 Impact of Label Overlap Ratio ρ

The overlap ratio, ρ , as defined in our partitioning algorithm, controls the degree of shared labels between adjacent player partitions. This design parameter mediates the trade-off between player specialization (low ρ) and inter-player knowledge transfer (high ρ).

Experimental Setup. To analyze this trade-off, we have fixed $N = 3$ and other hyperparameters to their optimal values. We varied the overlap ratio ρ across the range $[0.0, 0.1, 0.2, 0.3, 0.4, 0.5]$, where $\rho = 0$ corresponds to a disjoint (hard) partitioning of the label space. We evaluated the impact on both mAP and Rare-F1.

Results and Analyses. The experimental outcome, detailed in Table 2, validates the necessity of controlled overlap. At $\rho = 0$, where players operate on completely disjoint label sets, performance is significantly degraded. This demonstrates that without a shared vocabulary at the partition boundaries, knowledge transfer is inhibited. As ρ increases to a moderate value of 0.2, both mAP and Rare-F1 show a marked improvement. This confirms our hypothesis that controlled redundancy is essential for the system to learn robust representations for all labels. Beyond this optimal point, increasing ρ further leads to diminishing returns, as excessive overlap reduces the incentive for specialization and undermines the core "division of labor" principle.

Table 5: Sensitivity analyses on the label overlap ratio ρ on Pascal VOC 2007. Results are reported as mean \pm std over 3 runs. Best performance is in bold.

Overlap Ratio (ρ)	mAP (%)	Rare-F1 (%)
0.0	91.5 ± 0.4	75.8 ± 0.6
0.1	92.3 ± 0.3	78.5 ± 0.4
0.2	92.6 ± 0.2	79.3 ± 0.3
0.3	92.5 ± 0.3	79.1 ± 0.3
0.4	92.4 ± 0.3	78.9 ± 0.4
0.5	92.4 ± 0.4	78.8 ± 0.4

Received 20 February 2007; revised 12 March 2009; accepted 5 June 2009